Targeting cellular gaps using Janus nanoparticles containing cationic polymers and surfactant lipids

Akihiro Matsumoto[1,*,§], Takeo Kitazawa[2,§], Yuta Hatori[2], Hiroshi Nakanishi[2],
Chie Watanabe[3], Tomoya Takashima[1], Masahiro Murakami[1]

[1] Laboratory of Pharmaceutics, Faculty of Pharmacy, Osaka Ohtani University, Osaka, Japan;
[2] Yasuda Women's University, Hiroshima, Japan;
[3] Laboratory of Clinical Pathology, Faculty of Pharmacy, Josai University, Saitama, Japan.

SUMMARY Since nanoparticles are taken up into cells by endocytosis, phagocytosis, or pinocytosis, they have been studied as intracellular drug carriers. Janus particles have an anisotropic structure composed of two or more distinct domains and have been proposed for use in various applications, including use as imaging agents or nanosensors. This study aimed to clarify the influence of the type of nanoparticles on their distribution in a human Caucasian colon adenocarcinoma (Caco-2) cell monolayer. We fabricated Janus and conventional spherical nanoparticles composed of pharmaceutically applicable ingredients. Janus and spherical nanoparticles composed of a cationic polymer and surfactant lipids were prepared by controlling the solvent removal pattern from the oil phase in the solvent removal process using the solvent evaporation and solvent diffusion methods. The distribution of nanoparticles in the Caco-2 cell monolayer was then evaluated using confocal laser microscopy. The mean hydrodynamic size of the fabricated Janus nanoparticles was 119.2 ± 4.6 nm. Distribution analysis using Caco-2 cells suggested that Janus nanoparticles were localized around the adherens junctions located just below the tight junction. Clear localization was not observed in non-Janus nanoparticles with the same composition. The clear localization of the Janus nanoparticles around the adherens junction may be due to their positive charge and asymmetric structure. Our results suggest the considerable potential for the development of nanoparticulate drug carriers to target cellular gaps.

Keywords human Caucasian colon adenocarcinoma (Caco-2) cell, adherens junction, cationic polymer, surfactant lipids, cellular uptake

1. Introduction

Recently, nanoparticles have been used for medical purposes as nanomedicines. They have been investigated as drug carriers for intracellular delivery because they can be taken up into target cells by endocytosis, phagocytosis, or pinocytosis. The first step in cellular uptake is the attachment of particles to the cell membrane. This is influenced by the characteristics of the nanoparticles, such as charge and size (*1-7*). In addition to these properties, the structure of the particles influences their attachment to cell membranes (*1,4,6,7*). Moreover, all the forementioned attributes are cardinal for phagocytic internalization (*1,6*).

Janus particles are representative heterogeneous particles, which have an anisotropic structure composed of two or more distinct domains. They have been proposed for use in various applications, including their

use as catalysts (*8,9*), imaging agents or nanosensors (*8,10*), and excipients in cosmetics (*8*). They also exhibit various configurations (*11-13*), including dumbbell, hamburger, spherical, and snowmen structures (*14*). Recently, various medical applications of Janus particles have been proposed. One such proposal involves the application of multiple containments within a Janus particle. For example, Janus particles can achieve dual loading and release of drugs (*15*), which conventional monolithic particles cannot. The distinct domains of Janus particles have different properties, such as being hydrophobic/hydrophilic (*16*) and cationic/anionic (*17*). Hence, these particles can encapsulate specific drugs with different properties in distinct domains or independently release each drug after a different trigger, such as heat (*18*) and light (*19*). We reported that both hydrophobic and hydrophilic fluorescent substances could be encapsulated into Janus microspheres (*20*). Janus particles can also

have separate functions in their distinct domains, including drug-loading and targeting domains. Polymer-magnetic Janus particles can have separate functions in three compartments, that is, anti-tumor drug, magnetic, and fluorescence regions for killing cancer cells, target location, and fluorescence tracing, respectively (*21*). In addition to these applications for drug delivery systems, Janus particles have also been investigated for bio-sensing technologies (*22*).

Another development direction for Janus particles is utilizing their orientational properties, which can occur between particles or particles and membranes. These orientational interactions are a unique property of Janus particles and cannot be achieved using conventional monolithic particles. The orientation between particles is referred to as self-assembly, which can build unique structures (*23-25*). Regarding the orientation of attached particles on a membrane, it has been reported that hollow microtubes can be formed by designing two biologically distinguishable regions: one exhibiting high binding affinity for cells and the other being essentially resistant to cell binding (*26*). In our previous study, orientational attachment on the human Caucasian colon adenocarcinoma (Caco-2) cell membrane was confirmed using Janus-type microspheres composed of a cationic polymer and hard fat (*20*). We found that the Janus microspheres had unique orientation properties in that the cationic side was in contact with the surface of the Caco-2 cell membrane while the lipid side faced the gastrointestinal lumen. This suggests that Janus microspheres are mucoadhesive drug carriers that are not affected by digestive enzymes, which is useful for improving enteral drug absorption by increasing drug retention. However, since Janus microspheres are too large to be taken up by Caco-2 cells and remain on the cell membrane surface, they cannot be used as drug carriers for intracellular delivery. Meanwhile, it has been reported that liposomes and polymeric micelles containing nucleic acids such as small interfering RNA (siRNA), which has low cellular uptake due to its anionic and highly hydrophilic properties, were incorporated into cells by endocytosis (*27,28*). Furthermore, these nanomedicines efficiently allowed siRNA to migrate to the cytoplasm while avoiding endosomal-lysosomal degradation (*27,28*). However, the cell surface dynamics and intracellular distribution of Janus nanospheres, which were prepared by reducing the size of Janus microspheres to facilitate cellular uptake, have not yet been elucidated, and their application as drug carriers for intracellular delivery has not been investigated.

In this study, we first fabricated nanoparticles and investigated the distribution of Janus nanoparticles in the Caco-2 monolayer. Aiming for future use as a delivery system for gastrointestinal absorption of drugs, we used pharmaceutically applicable ingredients for the fabrication of Janus nanoparticles, such as ethyl prop-2-enoate, methyl 2-methylprop-2-enoate, and

trimethyl-[2-(2-methylprop-2-enoyloxy) ethyl] azanium chloride (Eudragit® RSPO; Eudragit) and 2-[2,3-bis(2-hydroxyethoxy) propoxy] ethanol, hexadecanoic acid, and octadecanoic acid (Labrafil® M2130CS; Labrafil). We also evaluated the influence of particle structure on Caco-2 intracellular distribution of two types of nanoparticles, Janus and non-Janus. These two types of nanoparticles had the same formulation composition and were prepared by controlling the solvent removal pattern of the oil phase during the solvent removal process, using either the solvent evaporation or diffusion methods. The intracellular distribution of these nanoparticles in Caco-2 cells was analyzed with confocal laser microscopy. Our study findings could potentially focus nanomedicine research on the application of Janus nanoparticles in a new direction.

2. Materials and Methods

2.1. Materials

Eudragit was purchased from Evonik Industries AG (Essen, Germany), while Labrafil was gifted by Gattefossé (Lyon, France). Polyvinyl alcohol (PVA; JP03) was obtained from JAPAN VAM & POVAL Co., Ltd. (Osaka, Japan). Nile Red was purchased from Nacalai Tesque (Kyoto, Japan). A water-soluble, 4′,6-diamidino-2-phenylindole (DAPI)-containing compound (DAPI Fluoromount-G®) was purchased from Southern Biotech (Birmingham, AL, USA). Alexa Fluor™ 488-conjugated mouse monoclonal anti-zonula occludens-1 (ZO-1) antibody (ZO1-1A12; 339188) was purchased from Thermo Fisher Scientific (Waltham, MA, USA). Dulbecco's modified Eagle's medium (DMEM) and Dulbecco's phosphate-buffered saline (D-PBS) were purchased from FUJIFILM Wako Chemical Corporation, Ltd. (Osaka, Japan). Fetal bovine serum (FBS) was purchased from Nichirei Biosciences, Inc. (Tokyo, Japan). All other chemicals used were of reagent grade.

2.2. Cell lines and cell culture

Caco-2 cells were acquired from Dr. Nonaka (Yasuda Women's University). The cells were routinely incubated and maintained in DMEM supplemented with 10% FBS, 50 U/mL penicillin, and 50 µg/mL streptomycin at 37 °C in a humidified atmosphere containing 5% CO_2.

2.3. Observation of phase separations and viscosity measurement

Mixtures of Eudragit and Labrafil (1:2 w/w) were dissolved in methylene chloride or acetone. The solvent was slowly evaporated at 25°C until phase separation was observed. The resulting solution was then weighed to calculate the concentrations of the mixtures. For phase separation at the micro-scale, the mixture was

dropped on a glass slide, mounted with a cover glass, and observed using an optical microscope (Motic BA210E, Shimazu Rika Co., Ltd., Tokyo, Japan). The viscosities of the phase-separated solutions were measured using a rotational rheometer (LVDV-I Prime; AMETEK Brookfield Inc., Middleboro, MA, USA).

2.4. Fabrication of nanoparticles

Four types of nanoparticles were fabricated by the following method (Figure 1).

(*i*) Janus nanoparticles and sole Eudragit nanoparticles (method A)

Janus nanoparticles were fabricated using an oil-in-water (o/w)-type emulsion-solvent evaporation method. Here, 60 mg of Eudragit and 120 mg of Labrafil (for Janus particles) or 180 mg Eudragit (for sole Eudragit nanoparticles) were dissolved in 0.01% Nile Red-methylene chloride (1.5 mL) to prepare the oil phase. The resulting oil phase was emulsified in 0.001 M HCl-10% PVA-60% propylene glycol (5 mL) at 20,000 rpm using a homogenizer (ULTRA-TURRAX T18; IKA®-Werke GmbH & Co. KG, Staufen im Breisgau, Germany) for 5 min at 20-23°C. The resulting o/w emulsion was added to 100 mL of water, and the diluted emulsion was stirred at 20-23°C for 120 min to remove the solvent. This process was referred to as solvent evaporation. The obtained nanoparticle suspension was then washed, suspended in 0.01 μM HCl, and concentrated *via* ultrafiltration technique using a 100 kDa filter. The Eudragit and Labrafil particles fabricated using this method were encoded as formulation ID 'NJ' (Nano Janus; NJ) because they showed a Janus structure in nano-order. Furthermore, the sole Eudragit particles were encoded as formulation ID 'NC' (Nano Cation; NC) because they showed a cationic property in nano-order.

(*ii*) Eudragit -Labrafil non-Janus nanoparticles (method B)

Non-Janus nanoparticles were fabricated using the solvent-diffusion method. In this method, 60 mg Eudragit and 120 mg Labrafil were dissolved in 0.002% Nile Red-acetone (10 mL) to prepare the oil phase. The resulting oil phase was poured into 0.5% PVA-0.1 M phosphate buffer solution (pH 8.0) 200 mL under constant stirring. The resulting mixture was stirred, and the solvent evaporated under airflow. The obtained nanoparticles were washed, resuspended in 0.1 M phosphate buffer solution (pH 8.0), and concentrated *via* ultrafiltration using a 100 kDa filter. The particles fabricated using this method were encoded as formulation ID 'NM' (Nano Mixture; NM) because Eudragit and Labrafil were mixed to form particles, unlike Janus nanoparticles in which Eudragit and Labrafil were separated and localized.

(*iii*) Sole Labrafil nanoparticles (method C)

In this method, 180 mg Labrafil was dissolved in 0.01% Nile Red-methylene chloride (1.5 mL) and evaporated under airflow. The resulting mixture was melted at 80 °C, added to water at 80°C (15 mL), and sonicated for 1 min at 20 W using an ultrasonic homogenizer (BRANSON Sonifier SFX250, Emerson
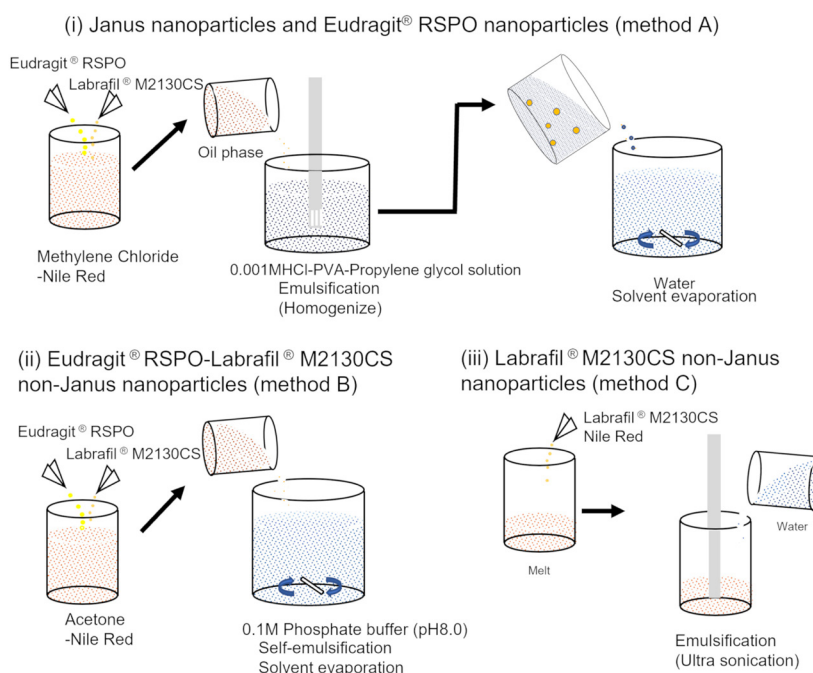

Figure 1. Scheme of the methods used for fabricating the four types of nanoparticles.

Electric Co. Ltd., St. Louis, MO, USA). The particles fabricated using this method were encoded as formulation ID 'NL' (Nano Lipid; NL) because they composed of lipids in nano-order.

2.5. Microscopic observations

The nanoparticles obtained were observed using scanning electron microscopy (SEM) (JSM-5500LV, JEOL Ltd., Tokyo, Japan). Samples for SEM observation were prepared by depositing gold-palladium at 15 mA for 30 s using ion sputtering equipment (Quick Auto Coater JFC-1500, JOEL Ltd., Tokyo, Tokyo, Japan). Samples were observed under the following conditions: accelerating voltage 15 kV, working distance 21 mm, and spot size 15 or 30.

2.6. Characterization of nanoparticles

The size of the nanoparticles was measured by Photon Correlation Spectroscopy using dynamic light scattering (DLS) (ELSZ-2, Otsuka Electronics Co. Ltd., Hirakata, Japan). Water was used as the dispersion medium at 25°C, and the sizes obtained from the DLS analyses were considered the hydrodynamic diameters. Zeta potential was measured using a zeta potential analyzer (ELSZ-2000Z, Otsuka Electronics Co., Ltd., Hirakata, Japan).

2.7. Distribution analysis of nanoparticles in a Caco-2 cell monolayer using immunocytochemistry

The Caco-2 cells were seeded on a porous Transwell filter membrane (cell culture insert, Transparent polyethyleneterephthalate membrane, 24 wells, pore size = 0.4 μm, Corning Inc., New York, USA) at a density of 1×10^4 cells/well and cultured in DMEM containing 10% FBS, 50 U/mL penicillin, and 50 μg/mL streptomycin until a confluent monolayer was formed and its transepithelial electrical resistance (TEER) was approximately 1000 Ω cm^2. Each nanoparticle encapsulating Nile Red was suspended in DMEM supplemented with 10% FBS, 50 U/mL penicillin, and 50 μg/mL streptomycin. After the cells in the apical side of the well were washed with 0.5 mL DMEM with 10% FBS, 50 U/mL penicillin, and 50 μg/mL streptomycin at 37°C, a 0.5 mL aliquot of the resulting suspension with a nanoparticle concentration of 0.4 mg/mL was added to the apical side of each well. After incubation for 3 h at 37°C, the apical side of the well was carefully washed twice with D-PBS. Cells cultured on porous filter membranes were then fixed with 4% paraformaldehyde, permeabilized with 0.2% Triton X-100 in D-PBS, and blocked with 3% bovine serum albumin. After the porous filter membrane from which cells were cultured was separated from the Transwell using a cutter, the cells were incubated with Alexa Fluor™ 488-conjugated monoclonal anti-ZO-1 antibodies (4°C, overnight). The cells were then mounted using DAPI Fluoromount-G ZO1, a tight junction protein, then the nucleus and nanoparticles in each cell were visualized *via* confocal laser microscopy using a FV1000 microscope (Olympus Co., Ltd., Tokyo, Japan). Images were processed using ImageJ software (*29*) with the Fiji package (*30*).

2.8. Statistical analysis

All experiments were performed in triplicate and the results are presented as mean ± standard deviation.

3. Results

3.1. Phase separation between Eudragit and Labrafil

The phase separation between Eudragit and Labrafil (1:2, w/w) in methylene chloride was observed at 1128 ± 0.3 mg/g at 25°C. Microscopy images of the phase separation and deposition on the surface of the Eudragit -Labrafil (1:2, w/w)-methylene chloride solution is shown in Figure 2. The viscosity of the oil phase of Eudragit -Labrafil (1:2, w/w) at the phase separation point was 54 ± 0.0 mPa·s.

Figure 2. Optical micrograph of the Eudragit® RSPO-Labrafil® M2130CS methylene chloride solution. Phase status after 1 d of drying. The ratio of Eudragit® RSPO/Labrafil® M2130CS was 1:2 (w/w). The scale bar indicates 50 μm.

3.2. Characteristics of nanoparticles

The nanoparticles composed of Eudragit -Labrafil were fabricated using two distinct methods, viz. solvent diffusion and solvent evaporation. The structures of the fabricated nanoparticles are shown in Figure 3 and summarized in Table 1. The Eudragit -Labrafil nanoparticles (NJ01) fabricated using the solvent evaporation method showed a Janus-type structure (Figure 3a), which was independent of Nile Red loading (NJ03) or particle size (NJ02). In contrast, the sole Eudragit (NC01) and sole Labrafil (NL01) nanoparticles had a non-Janus spherical structure. Similarly, Eudragit -Labrafil nanoparticles (NM01) fabricated using the solvent diffusion method showed a non-Janus spherical structure (Figure 3b).

The other particle characteristics are summarized in Table 1. Two Janus nanoparticle formulations with different hydrodynamic diameters (the diameter of NJ01 was smaller than that of NJ02) were prepared by adjusting the PVA concentration and stirring speed during emulsification. The measured hydrodynamic diameters of all formulations aligned with the sizes determined *via* SEM, as shown in Figure 3. The hydrodynamic diameters of the spherical Eudragit -Labrafil nanoparticles (NM01) and sole Labrafil nanoparticles (NL01) were larger than those of the smaller Janus (NJ01) and sole Eudragit nanoparticles (NC01); however, their sizes corresponded to those of the larger Janus particles (NJ02).

Table 1 shows the ζ potential of each nanoparticle. The ζ potentials of the sole Eudragit nanoparticles (NC01) and sole Labrafil nanoparticles (NL01) were positive and negative, respectively. Janus nanoparticles (NJ02) were approximately 300 nm in size and were comparable in charge to sole Eudragit nanoparticles (NC01). Small Janus nanoparticles (NJ01) showed a lower ζ potential than larger Janus nanoparticles (NJ02), with a persistently stronger charge than that of non-Janus nanoparticles (NM01).
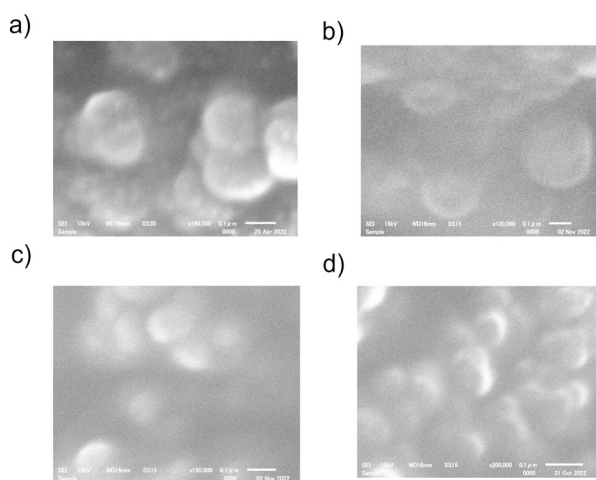
3.3. Distribution of nanoparticles in Caco-2 cell monolayers

The following five nanoparticle formulations encapsulating the fluorescent dye Nile Red were added to the confluent Caco-2 cell monolayers: Janus nanoparticles (NJ01 and NJ02; the diameter of NJ01 was smaller than that of NJ02) and non-Janus nanoparticles (NM01, NC01, NL01). The distribution of these nanoparticles after 3 h of incubation with the Caco-2 cell monolayers was analyzed *via* confocal laser scanning

Figure 3. Scanning electron micrograph of nanoparticles. a) Eudragit® RSPO-Labrafil® M2130CS nanoparticles prepared using the solvent evaporation method, method A (NJ01); The ratio of Eudragit® RSPO/Labrafil® M2130CS was 1:2 (w/w). **b)** Eudragit® RSPO-Labrafil® M2130CS nanoparticles prepared using the solvent diffusion method, method B (NM01); The ratio of Eudragit® RSPO/Labrafil® M2130CS was 1:2 (w/w). **c)** Eudragit® RSPO nanoparticles prepared using the solvent evaporation method, method A (NC01). **d)** Labrafil® M2130CS nanoparticles prepared by ultrasonicating the suspension in water, method C (NL01).

Table 1. Characteristics of the fabricated nanoparticles

Formulation No.	Structure	Composition	Nile Red	Fabrication method	ζ potential (mV)		Hydrodynamic diameters (nm)		Polydispersity index	
					mean	S.D.	mean	S.D.	mean	S.D.
NJ01	Janus	Eudragit RSPO: Labrafil M2130CS =1:2	+	Method A	+29.0	8.2	119.2	4.6	0.183	0.057
NJ02	Janus	Eudragit RSPO: Labrafil M2130CS =1:2	+	Method A[*)]	+41.9	1.8	310.7	5.6	0.183	0.001
NJ03	Janus	Eudragit RSPO: Labrafil M2130CS =1:2	-	Method A	+26.4	5.4	140.1	4.3	0.211	0.072
NM01	Non-Janus (spherical)	Eudragit RSPO: Labrafil M2130CS =1:2	+	Method B	+11.7	1.6	300.4	25.9	0.232	0.029
NC01	Non-Janus (spherical)	Eudragit RSPO	+	Method A	+38.0	5.0	165.8	33.1	0.208	0.029
NL01	Non-Janus (spherical)	Labrafil M2130CS	+	Method C	-32.0	8.8	263.0	34.4	0.243	0.024

Data represents mean ± S.D. (n = 3 batches); [*]Emulsification condition was adjusted; water phase 2.5% PVA-60% propylene glycol, emulsification speed 2000 rpm using a propeller mixer.

microscopy (Figure 4). Janus nanoparticle formulations were localized both inside and outside the cells near the adherens junction, which were closer to the basement membrane than the tight junction. In contrast, non-Janus nanoparticles (NM01), which consisted of Eudragit and Labrafil, were more widely distributed in the cytosol than Janus nanoparticle formulations (NJ01, 02) and strongly aggregated in cells despite having the same composition.

Herein, we investigated whether the localization of the two Janus nanoparticle formulations (NJ01, 02), near the adherens junction, was due to their strong positive ionic charge or Janus structure. Spherical nanoparticle formulations, consisting only of the cationic polymer Eudragit (NC01) and only Labrafil (NL01), were prepared and added to a Caco-2 cell monolayer, and their intracellular distributions were analyzed. Nanoparticle formulation NC01 (ζ potential: +38.0 mV), containing nanoparticles with a large ζ potential composed only of the cationic polymer Eudragit, also tended to be localized near the adherens junction on the basal membrane side of the tight junction. Moreover, no aggregation was observed, showing a similar tendency to that of nanoparticle formulations NJ01 and NJ02. However, they were distributed in the cytoplasm at the height of the Z-position where ZO-1, a tight junction marker, differed from Janus particles. In contrast, nanoparticle formulation NL01 (ζ = -32.0 mV), which was composed

solely of the lipid Labrafil and had a negative ζ potential, was distributed within cells. Moreover, this formulation was observed to have strong particle aggregation and was not distributed outside the cells near the adherens junction, similar to that of the spherical nanoparticle formulation NM01. In addition, because nanoparticle formulation NL01 consisted only of lipids with a low softening point, it was assumed that it strongly aggregated in the cytoplasm after being taken up by cells.

4. Discussion

To investigate the distribution of nanoparticles in cells, their physicochemical properties, including their structure, must be controlled. The structure of the particles is considered to be influenced by the speed of solvent removal from the oil phase into the water phase. In the solvent diffusion process, solvent removal was rapid that Labrafil and Eudragit simultaneously solidified and formed spherical nanospheres. In contrast, the solvent evaporation process takes more time to remove the solvent from the oil phase in the emulsion. In this method, phase separation between Eudragit and Labrafil has to be considered during solvent evaporation. We previously reported that the shape of the resultant particles depends on solvent removal speed (*31*). The relationship between Janus particle formation, phase
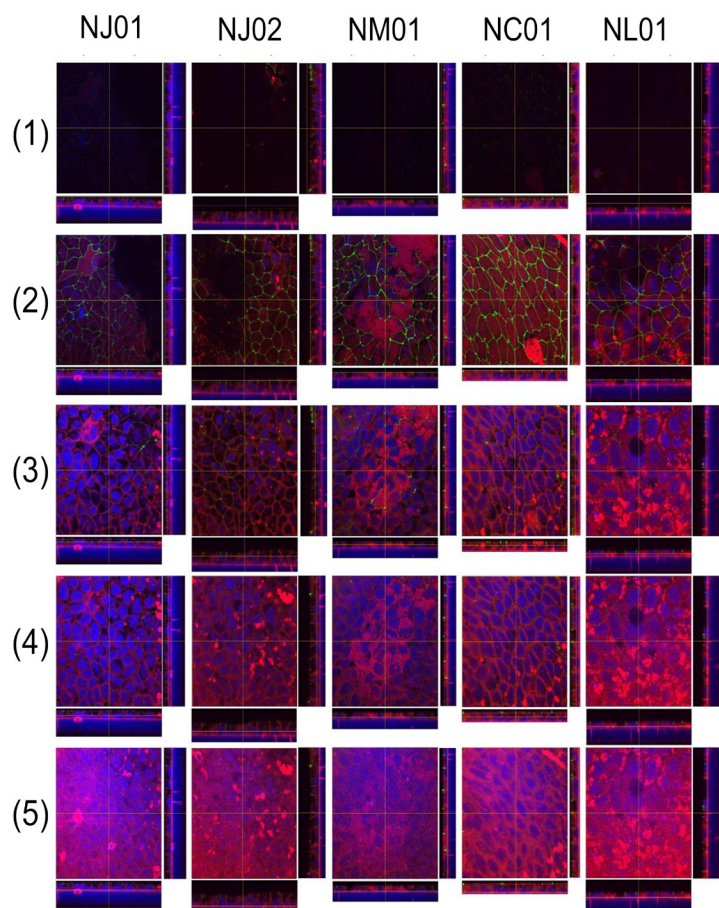

Figure 4. Distribution of nanoparticle formulations within Caco-2 cell monolayers. Five nanoparticles were used, including small Janus nanoparticles of Eudragit® RSPO-Labrafil® M2130CS (NJ01; the ratio of Eudragit® RSPO/Labrafil® M2130CS was 1:2 [w/w]), large Janus nanoparticles of Eudragit® RSPO-Labrafil® M2130CS (NJ02), non-Janus particles of Eudragit® RSPO-Labrafil® M2130CS (NM01; the ratio of Eudragit® RSPO/Labrafil® M2130CS was 1:2 [w/w]), Eudragit® RSPO nanoparticles (NC01), and Labrafil® M2130CS nanoparticles (NL01). Confocal laser microscopy images of Caco-2 cells after 3 h of incubation with each particle (0.2 mg/well). The confocal micrographs represent a three-dimensional analysis of five different optical sections (Z-axis) of the cells as follows: (1) apical membrane, (2) tight junction, (3) adherens junction (closer to the apical membrane), (4) adherens junction (closer to the basal membrane), and (5) basal membrane. The red dots, green lines, and blue spheres indicate nanoparticles stained by Nile Red, tight junctions, and nuclei, respectively.

separation, solvent removal speed, and the viscosity of the oil phase is illustrated in Figure 5.

In the solvent evaporation method, phase separation is supposed to occur in the oil phase at a certain time during the solvent evaporation process. To form a Janus structure, the separated droplets must migrate to the surface of the oil phase in the emulsion during solvent evaporation. The viscosity of the oil phase is important for migration of the separated droplets. The viscosity of the oil phase at the phase separation point between the two materials should not be high enough to separate easily into two layers. In addition, the Janus structure must be maintained after migration. Therefore, the appropriate solvent removal speed is important for maintaining the Janus structure. In this study, the appropriate solvent removal rate was obtained from the volume of the water phase to that of methylene chloride. To this end, we fixed 100 mL as the volume of the water phase in the solvent evaporation process, which provided approximately 1.5 times the saturated solubility (1.3 g/100 mL at 20℃) for the methylene chloride applied in our previous study (*20*).

The structure of particles consisting of two components (1 and 2) is also considered to be influenced by interfacial tension (*32,33*). The role of interfacial tension in nanoparticle structure is illustrated in Figure 6. If phase separation occurs between components 1 and 2 in the oil phase during an o/w type emulsion solvent evaporation, a triple junction comprising components 1- and 2-rich phases in an oil droplet and a water phase is assumed to form. Three interfacial tensions at the triple junction are also suggested to be a determinant of Janus particle formation. Because the Labrafil used in this study had hydrophilic surfactant action (HLB 9), it was assumed to have a sufficiently low surface tension to be in contact with the water phase. Similarly, Eudragit has an increased cationic charge and swells under acidic conditions. In this study, a slightly acidic water phase was used to reduce the interfacial tension between the water and the Eudragit phases for Janus particle formation because Eudragit retains considerable water
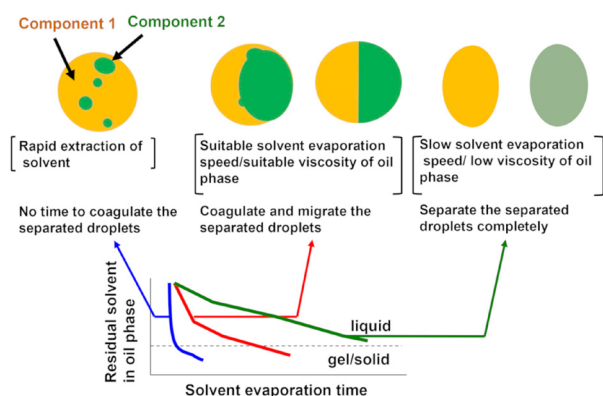
from swelling. In addition, acidic conditions promoted swelling and protrusion of the Eudragit phase from the Labrafil layer, which precipitated out first. These factors promoted the formation of Janus nanoparticles. In contrast, in solvent diffusion, which produced Eudragit-Labrafil nanoparticles with non-Janus structures, the alkalinity (pH 8.0) of the external phase used in the fabrication process suppressed the swelling of Eudragit with a positive charge. This increased the interfacial tension between the water and Eudragit phases, and the protrusion of the Labrafil layer was suppressed.

Besides the structure of nanoparticles, charge is another important property because it can influence cell membrane attachment and cellular uptake. In this study, Eudragit and Labrafil, used as components of nanoparticles, had positive and negative charges, respectively. However, the Janus and non-Janus nanoparticles consisting of the two components had positive charges. The charge of Eudragit as a cationic polymer was due to its ionic property, whereas that of Labrafil, a non-ionic substance, was due to its dipole property. Generally, the dipole force is weaker than the
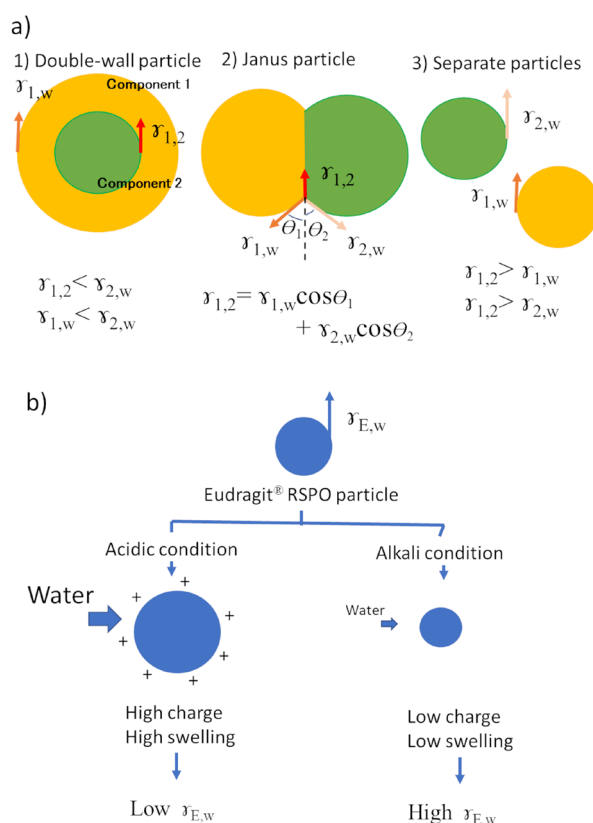

Figure 6. Theoretical image for the role of interfacial tension and swelling on particle structure. a) Effect of interface tension balance on particle structure. The arrows indicate the interfacial tension between components 1 and 2 (red: $\gamma_{1,2}$), between component 1 and external water phase (orange: $\gamma_{1,w}$), and between component 2 and external water phase (peach: $\gamma_{2,w}$). b) Effect of acidity and alkalinity in the external water phase on the interfacial tension of cationic polymers. The blue arrow indicates the interfacial tension between Eudragit® RSPO and the external water phase ($\gamma_{E,w}$).

Figure 5. Theoretical image of the influence of solvent evaporation speed on particle structure.

ionic force; therefore, a positive charge dominated on the spherical surface of the Janus particles composed of Eudragit and Labrafil. The non-Janus particles comprising Eudragit and Labrafil showed weaker ζ potentials than the sole Eudragit nanoparticles, indicating that Labrafil shields the positive charge of Eudragit. Complete shielding, similar to the coating of Labrafil over Eudragit, was not likely to occur because the charge of the spherical nanoparticles did not align with the charge of the sole Labrafil nanoparticles. In contrast, in the case of Janus nanoparticles, the positive charge of Eudragit was not shielded by Labrafil similar to non-Janus nanoparticles; therefore, the charge was stronger than that of non-Janus nanoparticles, and the intensity of the charge was comparable to that of sole Eudragit nanoparticles. This was due to the limited shielding at the joint between the two hemispheres.

Next, we investigated the distribution of Janus and non-Janus particles with the aforementioned properties in the intestinal membrane. Janus and non-Janus particles were added to Caco-2 cell monolayers. When the nanoparticles were added to the apical side of the Caco-2 monolayer at 4 mg/mL, as previously reported (*20*), fragmentation of the cell nuclei was observed. Therefore, subsequent nanoparticle incubation experiments were performed at a concentration of 0.4 mg/mL. Nuclear fragmentation was not observed at this concentration. Regarding the cytotoxicity of lipid nanoparticles, the cell viability after 24 h was approximately 70-100% after adding the nanoparticles at 0.4 mg/mL to Vero and L1210 cells (*34*). However, because the lipids and cells used in lipid nanoparticles and their incubation time with cells in this study differed from those in the previous report, further research is required to accurately determine the cytotoxicity of the Janus and non-Janus nanoparticles we used. As a result, unlike the Janus microparticles reported previously (average particle size: 30 μm) (*20*), the Janus nanoparticles of all formulations were taken up by Caco-2 cells. One of the reasons why all nanoparticles were incorporated into the cells could be because of their small particle size, which is known to influence cellular uptake (*6,7*). It has been reported that poly(DL-lactide-co-glycolide) particles (100 nm) were observed inside Caco-2 cells, whereas poly(DL-lactide-co-glycolide) particles larger than 300 nm were only associated with the apical membrane of Caco-2 cells (*35*). However, the results of our experiments suggest that nanoparticles with a diameter of up to 300 nm were taken up into cells, but further research is needed to determine the size threshold for cellular uptake of the carriers.

The main results presented here suggest that the unique intracellular distribution of Janus nanoparticle formulations, which were localized near the adherens junction, was in part due to a strong positive charge. For the non-Janus nanoparticles, the incorporated spherical nanoparticles were distributed throughout the cytosol, which is similar to findings in a previous report (*35*).

The nanoparticles of the cationic polymer (NC01) were distributed in the cytoplasm at the height of the tight junction. However, they tended to be distributed near the adherens junction, in contrast to Janus particles. According to these observations, the distribution of Janus particles near the adherens junction may have been due to its positive charge. Meanwhile, the distribution of Janus particles (NJ01, 02) in the cytoplasm at the height of the tight junction was suppressed, which was unique in Janus nanoparticles. Although this may have been due to the Janus structure, further investigation is needed.

Additionally, in this study, there was a difference in the aggregation of Janus and non-Janus nanoparticles in the cell membrane. Non-Janus nanoparticles (NM01) exhibited intracellular aggregation, which was attributed to their low ζ potential (+11.7 mV) due to the shielding of the cationic polymer by the surfactant lipids as mentioned above. Janus nanoparticles had higher ζ potentials. These results suggest that these particles were highly cationic, effectively preventing aggregation.

Unlike conventional lipid nanoparticles, which tend to go to endosomes and lysosomes after cellular uptake by endocytosis or phagocytosis, one way to utilize the unique intracellular distribution of our reported Janus nanoparticles in the cellular gap near the adherens junction can be to use them as drug carriers for the treatment of disorders such as Alzheimer's and inflammatory bowel diseases. Recently, it has been reported that proteases "gingipains" secreted by periodontal disease bacteria "*Porphyromonas gingivalis*" may destroy the blood-brain barrier and cause the progression of Alzheimer's disease (*36*). Furthermore, in inflammatory bowel diseases, such as Crohn's disease and ulcerative colitis with intestinal hemorrhage, free heme released from red blood cells impairs the barrier function of gastrointestinal epithelial cells, further worsening the condition (*37,38*). As a fundamental treatment for such diseases in which barrier disruption of endothelial or epithelial cells is involved in development and progression, we suggest a new method to repair barrier functions by delivering drugs to cellular gaps using Janus nanoparticles containing cationic polymers and surfactant lipids.

In future studies, we will investigate how the Janus nanoparticle formulations, which have cationic surfaces of their Janus structure, interact with cellular gap-related proteins, such as E-cadherin and nectin, to elucidate their detailed intracellular distribution mechanism. E-cadherin and nectin are transmembrane proteins that are bound to actin filaments, forming the cytoskeleton in the cytoplasm near the adherens junction (*39*).

In conclusion, Janus particles were fabricated using the cationic polymer, Eudragit, and lipid, Labrafil. The hydrodynamic size of the fabricated Janus nanoparticles was approximately 100 nm. Distribution analysis of the nanoparticles in Caco-2 cell membrane suggested that the Janus nanoparticles were localized in the adherens

junction and the cytosol near the adherens junction, which is just below the tight junction. Localization was not observed in spherical nanoparticles with the same composition. The clear localization of the Janus nanoparticles around the adherens junction may be due to their positive charge and asymmetric structure. The ability of our Janus nanoparticles to target cellular gaps can lead to their clinical application in the treatment of disorders related to cellular gaps, such as Alzheimer's disease and inflammatory bowel diseases. Although further investigation is needed to elucidate the localization of EudragitLabrafil Janus nanoparticles and suggest possible clinical applications, the present results present considerable potential for the development of nanoparticulate drug carriers to target cellular gaps.

Acknowledgements

Conflict of Interest: The authors have no conflicts of interest to disclose.

References

1. Salatin S, Yari Khosroushahi AY. Overviews on the cellular uptake mechanism of polysaccharide colloidal nanoparticles. J Cell Mol Med. 2017; 21:1668-1686.
2. Chuah LH, Roberts CJ, Billa N, Abdullah S, Rosli R. Cellular uptake and anticancer effects of mucoadhesive curcumin-containing chitosan nanoparticles. Colloids Surf B Biointerfaces. 2014; 116:228-236.
3. Li Q, Liu CG, Yu Y. Separation of monodisperse alginate nanoparticles and effect of particle size on transport of vitamin E. Carbohydr Polym. 2015; 124:274-279.
4. Jo DH, Kim JH, Lee TG, Kim JH. Size, surface charge, and shape determine therapeutic effects of nanoparticles on Brain and Retinal Diseases. Nanomedicine. 2015; 11:1603-1611.
5. De Jong WH, Borm PJ. Drug Delivery and Nanoparticles: Applications and hazards. Int. J. Nanomedicine. 2008; 3:133-149.
6. Salatin S, Maleki DS, Yari Khosroushahi A. Effect of the surface modification, size, and shape on cellular uptake of nanoparticles. Cell Biol Int. 2015; 39:881-890.
7. Doshi N, Mitragotri S. Macrophages recognize size and shape of their targets. PLOS ONE. 2010; 5:e10051.

8. Lee KJ, Yoon J, Lahann J. Recent advances with anisotropic particles. Curr Opin Coll Interface Sci. 2011; 16:195-202.
9. Cobo S, Heidkamp J, Jacques PA, Fize J, Fourmond V, Guetaz L, Jousselme B, Ivanova V, Dau H, Palacin S, Fontecave M, Artero VA. A Janus cobalt-based catalytic material for electro-splitting of water. Nat Mater. 2012; 11:802-807.
10. Zhang Q, Zhang L, Li S, Chen X, Zhang M, Wang T, Li L, Wang C. Designed synthesis of Au/Fe3O4@C Janus nanoparticles for dual-modal imaging and actively targeted chemo-photothermal synergistic therapy of cancer cells. Chemistry. 2017; 23:17242-17248.
11. He J, Hourwitz MJ, Liu Y, Perez MT, Nie Z. One-Pot facile synthesis of Janus particles with tailored shape and functionality. Chem Commun. 2011; 47:12450-12452.
12. Kuijk A, van Blaaderen A, Imhof A. Synthesis of monodisperse, rodlike silica colloids with tunable aspect ratio. J Am Chem Soc. 2011; 133:2346-2349.
13. Zhao R, Yu X, Sun D, Huang L, Liang F, Liu Z. Functional Janus particles modified with ionic liquids for dye degradation. ACS Appl Nano Mater. 2019; 2:2127-2132.
14. Su H, Hurd Price CA, Jing L, Tian Q, Liu J, Qian K. Janus particles: design, preparation, and biomedical applications. Mater Today Bio. 2019; 4:100033.
15. Dehghani E, Salami-Kalajahi M, Roghani-Mamaqani H. Simultaneous two drugs release form Janus particles prepared *via* polymerization-induced phase separation approach. Colloids Surf B Biointerfaces. 2018; 170:85-91.
16. Li XM, Zhou L, Wei Y, El-Toni AM, Zhang F, Zhao DY. Anisotropic growth- induced synthesis of dual-compartment Janus mesoporous silica nanoparticles for bimodal triggered drugs delivery. J Am Chem Soc. 2014; 136:15086-15092.
17. Liu Z, Cui J, Zhan W. Dipolar Janus liposomes: formation, electrokinetic motion and self-assembly. Soft Matter. 2020: 16:2177-2184.
18. Mou FZ, Chen CR, Zhong Q, Yin YX, Ma HR, Guan JG. Autonomous motion and temperature-controlled drug delivery of Mg/Pt-poly(N-isopropylacrylamide) Janus micromotors driven by simulated body fluid and blood plasma. ACS Appl Mater Interfaces. 2014; 6:9897-9903.
19. Wu Y, Lin X, Wu Z, Möhwald H, He Q. Self-propelled polymer multilayer Janus capsules for effective drug delivery and light-triggered release. ACS Appl Mater Interfaces. 2014; 6:10476-10481.
20. Matsumoto A, Watanabe C, Murakami M. Janus microspheres for enhanced enteral drug delivery: preparation and orientated attachment to a Caco-2 monolayer. Drug Discov Ther. 2019; 13:343-353.
21. Feng Z-Qi, Yan K, Li J, Xu X, Yuan T, Wang T, Zheng J. Magnetic Janus particles as a multifunctional drug delivery system for paclitaxel in efficient cancer treatment. Mater Sci Eng C Mater Biol Appl. 2019; 104:110001.
22. Jurado-Sánchez B, Campuzano S, Pingarrón JM, Escarpa A. Janus particles and motors: unrivaled devices for mastering (bio)sensing. Mikrochim. Acta. 2021; 188:416.
23. Banik M, Sett S, Bakli C, Raychaudhuri AK, Chakraborty S, Mukherjee R. Substrate wettability guided oriented self assembly of Janus particles. Sci Rep. 2021; 11:1182.
24. Yan J, Bloom M, Bae SC, Luijten E, Granick S. Linking synchronization to self-assembly using magnetic Janus colloids. Nature. 2012; 491:578-581.
25. Chen Q, Whitmer JK, Jiang S, Bae SC, Luijten E, Granick

S. Supracolloidal reaction kinetics of Janus spheres. Science. 2011; 331:199-202.

26. Gilbert JB, O'Brien JS, Suresh HS, Cohen RE, Rubner MF. Orientation-specific attachment of polymeric microtubes on cell surfaces. Adv Mater. 2013; 25:5948-5952.

27. Castanotto D, Rossi JJ. The promises and pitfalls of RNA-interference-based therapeutics. Nature. 2009; 457:426-433.

28. Cabral H, Kataoka K. Progress of drug-loaded polymeric micelles into clinical studies. J Control Release. 2014; 190:465-476.

29. Schindelin J, Rueden CT, Hiner MC, Eliceiri KW. The Image J ecosystem: an open platform for biomedical image analysis. Mol Reprod Dev. 2015; 82:518-529.

30. Schindelin J, Arganda-Carreras I, *et al*. Fiji: An open-source platform for biological-image analysis. Nat Methods. 2012; 9:676-682.

31. Matsumoto A, Murao S, Matsumoto M, Watanabe C, Murakami M. Fabrication of Janus particles composed of poly (lactic-Co-glycolic) acid and hard fat using a solvent evaporation method. Drug Discov Ther. 2016; 10:307-313.

32. Pekarek KJ, Jacob JS, Mathiowitz E. Double-walled polymer microspheres for controlled drug release. Nature. 1994; 367:258-260.

33. Zhang H, Wang F, Nestler B. Janus droplet formation *via* thermally induced phase separation: a numerical model with diffusion and convection. Langmuir. 2022; 38:6882-6895.

34. Winter E, Dal Pizzol C, Locatelli C, Crezkynski-Pasa TB. Development and evaluation of lipid nanoparticles for drug delivery: study of toxicity *in vitro* and *in vivo*. J Nanosci Nanotechnol. 2016; 16:1321-1330.

35. Gaumet M, Gurny R, Delie F. Localization and quantification of biodegradable particles in an intestinal cell model: the influence of particle size. Eur J Pharm Sci. 2009; 36:465-473.

36. Dominy SS, Lynch C, Ermini F, *et al*. Porphyromonas gingivalis in Alzheimer's disease brains: evidence for disease causation and treatment with small-molecule inhibitors. Sci Adv. 2019; 5:eaau3333.

37. Akagi R. Role of heme oxygenase in gastrointestinal epithelial cells. Antioxidants. 2022; 11:1323.

38. Akagi R, Akagi M, Hatori Y, Inouye S. Prevention of barrier disruption by heme oxygenase-1 in intestinal bleeding model. Biol Pharm Bull. 2016; 39:1007-1012.

39. Indra I, Hong S, Troyanovsky R, Kormos B, Troyanovsky S. The adherens junction: a mosaic of cadherin and nectin clusters bundled by actin filaments. J Invest Dermatol. 2013; 133:2546-2554.

§These authors contributed equally to this work.
Address correspondence to:
Akihiro Matsumoto, Laboratory of Pharmaceutics, Faculty of Pharmacy, Osaka Ohtani University, 3-11-1 Nishikori-kita, Tondabayashi-shi, Osaka 584-0854, Japan.
E-mail: matumoaki@osaka-ohtani.ac.jp